Role of Atomic Multiplets in the Electronic Structure of Rare-Earth Semiconductors and Semimetals

Leonid V. Pourovskii,[1] Kris T. Delaney,[2] Chris G. Van de Walle,[3] Nicola A. Spaldin,[3] and Antoine Georges[1]

[1]*Centre de Physique Théorique, École Polytechnique, CNRS, 91128 Palaiseau, France*
[2]*Materials Research Laboratory, University of California, Santa Barbara, 93106-5121, USA*
[3]*Materials Department, University of California, Santa Barbara, 93106-5050, USA*

(Received 22 July 2008; published 2 March 2009)

We present a study of the effects of strong correlations in rare-earth pnictides, in which localized $4f$ states simultaneously retain atomiclike character and strongly influence the free-electron-like valence electron states. Using erbium arsenide as our example, we use a modern implementation of dynamical mean-field theory to obtain the atomic multiplet structure of the Er^{3+} $4f$ shell, as well as its unusually strong coupling to the electronic Fermi surfaces; these types of behavior are not correctly described within conventional electronic-structure methods. We are then able to explain the long-standing theoretical question of the quasisaturation of magnetization in an applied magnetic field, and to obtain the first quantitative agreement with experimental Shubnikov–de Haas frequencies of the Fermi-surface sheets.

DOI: 10.1103/PhysRevLett.102.096401 PACS numbers: 71.27.+a, 71.18.+y, 71.20.Nr, 71.70.−d

Most rare-earth pnictides (RE-V) are characterized by partially occupied, highly localized f shells which, in the solid, split into upper and lower Hubbard bands at relatively high energy. The partially occupied f states are also responsible for magnetic moments that order at low temperatures, usually through the weak RKKY interaction. The valence band (composed of pnictide p states) tends to overlap or align (with a very small band gap) with the conduction band (of rare-earth $5d$ states); the details depend sensitively on interactions of the valence states, through hybridization and exchange splitting, with the localized $4f$ states. Simultaneously treating these two types of states and their interactions is a major challenge for conventional electronic-structure theories.

While the sensitivity of the electronic structure is almost universal in the series of RE-V, a particularly dramatic example is provided by erbium arsenide (ErAs) which is a material that has recently been cited for an array of potential technological applications [1–4], e.g., to thermoelectricity [5] and solid-state THz emitters [6]. The low-energy electronic structure of ErAs consists of a conduction band of predominant Er $5d$ character and a valence band of As $4p$ character, the small energy overlap of which leads to simultaneous, free electron and hole carriers of a low density, yielding a semimetal. Calculations often rely on treating the $4f$ states as frozen atomic core electrons. Using this approach, calculations based on the local-density approximation (LDA) correctly result in a semimetal, but do not otherwise provide an accurate description of the electronic properties. The volume of the calculated FS pockets is approximately 3 times too large, leading to incorrect carrier concentrations and SdH frequencies [7,8] compared with accurate measurements [9–12].

In this Letter, we show that a proper treatment of the $4f$ shell provides a solution to these difficulties. Thus, we demonstrate that ErAs provides a remarkable example of the importance of the treatment of localized states, in which the electronic bands near the Fermi level act as a sensitive probe of the atomic physics associated with the $4f$ states. The findings herein have consequences for understanding the electronic structure of a large class of rare-earth compounds.

Our approach is based on the dynamical mean-field theory [13] (DMFT), combined [14–16] with LDA. The $4f$ shell is treated as that of an effective-atom self-consistently coupled to an environment describing the rest of the solid. From the Hamiltonian of this effective atom (which takes into account crystal-field effects, intra-atomic Coulomb interactions and the spin-orbit coupling), a many-body self-energy is computed within the Hubbard-I approximation [17] and inserted into the Green's function of the full solid. Self-consistency over the total charge density and the effective-atom parameters is implemented. The full description of our approach can be found in Ref. [18]. In the present work it was generalized to include the spin-orbit interaction as well as the full 4-index local Coulomb interaction matrix. The parameter $U = 7.94$ eV of the local Coulomb interaction on the Er $4f$ shell has been determined by constrained LDA calculations, while the Slater integrals $F^2 = 12.1$ eV, $F^4 = 8.4$ eV, and $F^6 = 6.7$ eV, which are known to be weakly dependent on the crystalline environment, have been taken from optical measurements on Er ions embedded in a LaF_3 host [19]. All our calculations have been carried out in the rock-salt structure at the ErAs experimental lattice parameter of 5.74 Å.

The ground-state of an isolated Er^{3+} ion ($4f^{11}5d^0$) is a 16-fold degenerate multiplet ${}^4I_{15/2}$ ($S = \frac{3}{2}$, $L = 6$, $J = \frac{15}{2}$). In a cubic crystal field and at zero magnetic field, this multiplet is expected to split into twofold degenerate Γ_6 and Γ_7 multiplets, as well as three fourfold degenerate Γ_8 multiplets [20]. At self-consistency and in the absence

of a magnetic field, the eigenstates of our effective-atom Hamiltonian (right inset of Fig. 1) follow this expectation, the obtained ground state being the Γ_7 multiplet. In order to simulate the effect of the external magnetic field applied in experiments we added the term $H\mu_B(2\hat{S}_z + \hat{L}_z)$ into the Hamiltonian. We note that in ErAs the intersite exchange is small resulting in a low T_N of 4.5 K. Moreover, even for $T < T_N$ ferromagnetic alignment of the Er local moments can be enforced by relatively weak fields of ~1 T [21]. Hence, we neglect the intersite exchange and consider the Er local moments to be ferromagnetically aligned in all SdH experiments, while the magnitude of the local moments varies with the external field. As an external magnetic field, H, is turned on, the ground-state of the Er $4f$ shell remains approximately Γ_7 for a wide range of fields and can be decomposed on eigenstates of J_z according to: $a^{(H)}_{13/2}|J_z = \frac{13}{2}\rangle + a^{(H)}_{5/2}|J_z = \frac{5}{2}\rangle + a^{(H)}_{-3/2}|J_z = -\frac{3}{2}\rangle + a^{(H)}_{-11/2}|J_z = -\frac{11}{2}\rangle$, where the coefficients a_{J_z} depend on magnetic field. The magnetic moment vs field curve (Fig. 1) displays an initial sharp rise due to the Zeeman splitting of the Γ_7 state, followed by a rather slow increase in the range from 5 to 120 T due to the progressive polarization of the Γ_7 state.

From magnetoresistance experiments [12], it was proposed that the magnetic moment is saturated at a value [21] $\sim 5.3\mu_B$ in fields above 10 T. Indeed, we find values ranging from $4.8\mu_B$ at $H = 5$ T to $5.6\mu_B$ at $H = 10$ T, in good agreement with experiment. However, our analysis shows that this is really a quasisaturation, with the moment "frozen" by the crystal field. Eventually, at a very high field $H \simeq 120$ T we predict an abrupt increase of the moment to $8.9\mu_B$ due to a symmetry-changing transition of the ground-state from Γ_7 to Γ_8.

It is interesting to contrast these findings to those of LDA + U. We performed LDA + U calculations using the same framework as for DMFT, including the spin-orbit interaction, with the exception that the Hubbard-I self-energy is substituted with a local self-energy corresponding to the rotationally invariant Hartree-Fock expression.

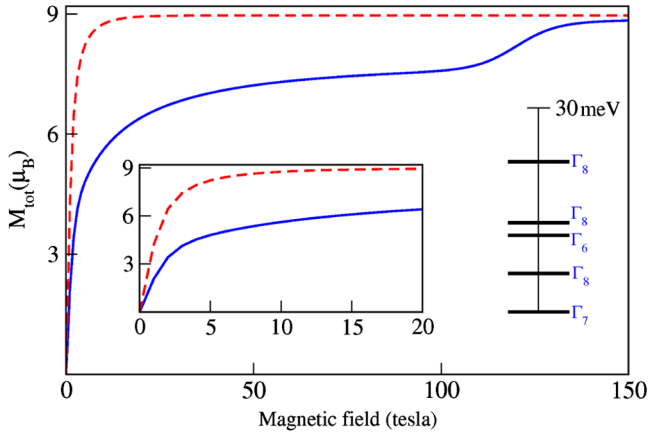

FIG. 1 (color online). Total magnetic moment on Er $4f$ shell, calculated with LDA + DMFT, vs applied magnetic field at $T = 4.2$ K with (solid line) and without (dashed line) crystal-field effects. The left inset magnifies the field range up to 20 T. The crystal field splitting of the $^4I_{15/2}$ multiplet in the zero-field paramagnetic ground state is shown in the right inset.

The calculations were performed for ferromagnetic ordering of the Er $4f$ spins. In the LDA + U approach [22], Coulomb interaction effects within the $4f$-shell are described by a self-consistent, orbital- and spin-dependent, *one-electron potential*. The lowest-energy LDA + U solution is found to correspond to the filling of independent electron levels according to Hund's rules [23], leading to the maximal spin and orbital moments consistent with a $4f^{11}$ shell. Indeed, our LDA + U calculations result in spin, orbital and total moments of $2.9\mu_B$, $6.0\mu_B$, and $8.9\mu_B$ respectively, in contradiction with the observed experimental value quoted above. Furthermore, as pointed out by Larson *et al.* for rare-earth nitrides [23], the LDA + U ground state breaks the cubic symmetry of the lattice because it is constructed by occupying one-electron eigenstates of the angular momentum operator $\hat{L}_z$. LDA + U solutions preserving cubic symmetry are obtained by occupying symmetry-adapted one-electron states (which are *not* eigenstates of $\hat{L}_z$), but they have higher energy. Hence, in an effective one-electron description, the system has to choose between minimizing the intra-atomic Coulomb interaction energy and preserving the lattice symmetry. In reality, however, this dilemma does not apply since atomic multiplets satisfy both requirements. A proper many-body treatment of atomic correlations avoids this conundrum, as demonstrated above.

We now describe the electronic structure of ErAs, obtained with LDA + U and LDA + DMFT (Fig. 2). Distinctive features corresponding to the $4f$ states are observed at high energy, corresponding to the upper- and lower- Hubbard bands (UHB/LHB). In LDA + DMFT, those "bands" truly are many-body excitations associated with the removal (LHB) or addition (UHB) of an electron in the $4f$ shell. The LHB spans the energy range ~ -11 eV to -5.5 eV, in good agreement with photoemission experiments [24,25]. Within LDA + DMFT the UHB consists of not only the main peak at 2–3 eV above the Fermi energy, but also additional multiplet peaks at ~3–4 eV. Discussed also for δ-Pu [26], this multiplet structure is responsible for the apparent width of the UHB, which we find to be ~1.5 eV in good agreement with inverse photoemission measurements [24,25].

In contrast, the UHB found with LDA + U spans an energy range of only ~0.75 eV, because the additional multiplet peaks are missed in this approach. Furthermore, a distinctive feature found within LDA + U is that the UHB is almost fully (minority) spin-polarized. This is clearly due to the maximal (Hund's rule) spin moment, corresponding to the complete filling of the $4f$ majority-spin states so that no electron addition is possible in the majority channel. In contrast, the UHB found within LDA + DMFT is found to be only partially polarized.

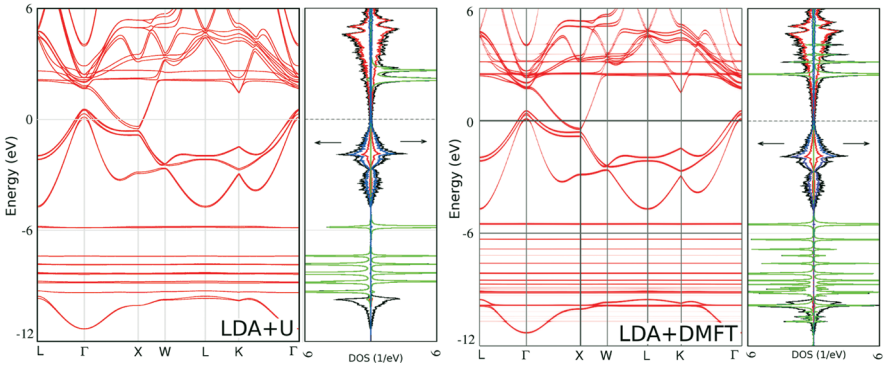

FIG. 2 (color). Band structure and density of states (DOS) of ErAs from LDA + U (left), and LDA + DMFT at an applied field of 5 T (right). In the DOS the total, Er 5d, Er 4f and As 4p states are displayed by the black, red, green, and blue lines, respectively.

Hence UHB transitions are possible in both spin channels, a distinctive prediction for possible spin-polarized photoemission experiments.

We now show that these differences in the description of the high-energy 4f states have key consequences for the electronic properties of states near the Fermi level. Near the Γ high-symmetry point, the As 4p bands form "heavy-" (*hh*) and "light-" (*lh*) hole pockets, as well as a small hole pocket (*sh*) due to the spin-orbit splitting of the 4p states, while the ellipsoidal electronic pocket at the X point is associated with the Er 5d states (Fig. 3).

As mentioned above, an LDA calculation treating the 4f shell as core states strongly overestimates the p-d overlap, and hence the carrier concentration and the size of the FS pockets. Both the LDA + DMFT and LDA + U treatment of the 4f states lead to a drastic reduction in the magnitude of the carrier density and SdH frequencies (Table I), and hence to a much better agreement with experiments. We note that self-consistency over the charge density within our LDA + DMFT approach leads to corrections in band positions, of the order of 400 meV, that prove to be important due to the scale of the band overlap in ErAs. These results demonstrate that taking into account interaction effects in the 4f shell is important for a proper description of the *valence* band structure. Previous works achieved a similar result through an empirical shift of the 5d band [8,28].

Despite similar overall reductions in the FS pocket volumes, the LDA + U and LDA + DMFT results differ significantly for the exchange splitting of these pockets. In Table II, we display the measured splittings [9,11,12] in SdH experiments along with the calculated values from LDA + DMFT, LDA + U and a recent spin-polarized GW work [27]. It is apparent that LDA + U (and spin-polarized GW) strongly overestimates the splitting of all orbits, especially for the hole pockets, while a much better agreement with experiments is obtained from LDA + DMFT. The reasons for this success are (i) a proper description of the crystal-field induced freezing of the 4f spin moment (in contrast to the full polarization obtained from LDA + U) and (ii) a proper description of the orbital angular momentum content of the upper Hubbard band. Electronic pockets are mainly sensitive to the first effect, since the direct hybridization between the Er d and f states is very small near the X point [8] so that the splitting of the electronic pocket is mostly due to the exchange field induced by the f states in the local charge density [29]. Because the spin polarization of the f states is strongly overestimated in

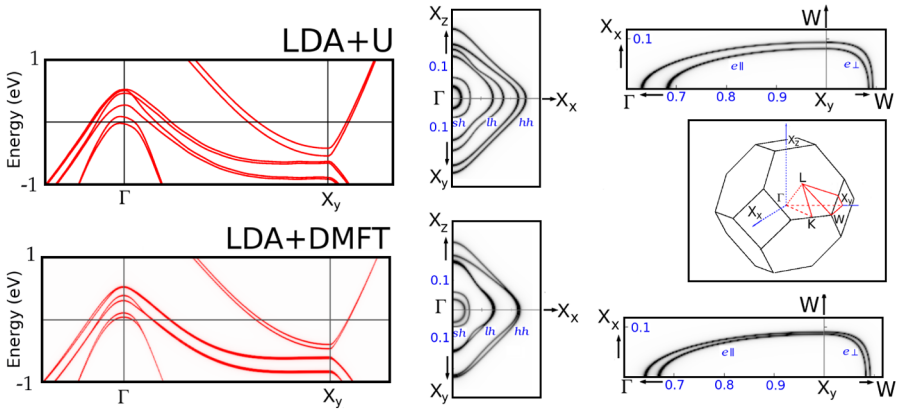

FIG. 3 (color online). The low-energy band structure of ErAs from LDA + U (top) and LDA + DMFT (bottom). The spin polarization, oriented along the z axis, lifts the cubic symmetry and leads to inequivalent band structures along the x, y and z axes. We therefore denote the X high-symmetry points as X_x, X_y, and X_z. The overlap of As 4p and Er 5d bands near E_F are shown on the left-hand side. To the right are the cross sections of the hole pockets at the Γ point in the xy and xz planes, followed by the longitudinal $e \parallel$ (in the $\Gamma X_y W$ plane) and transverse $e \perp$ ($X_y WW$ plane) cross sections of the electronic pocket. The exchange splittings of the pockets are clearly seen.

TABLE I. Shubnikov–de Haas (SdH) frequencies (in tesla) and carrier concentrations of electrons/holes n (in 10^{20} cm^{-3}). The frequencies f_{sh}, f_{lh}, and f_{hh} correspond to cross sections of the small, light, and heavy hole pockets near the Γ high-symmetry point, respectively. The frequencies $e \perp$ and $e \parallel$ are due to the transverse and longitudinal cross sections of the ellipsoidal electronic pocket. The experimental carrier concentrations and SdH frequencies are for an $Er_{0.57}Sc_{0.43}As$ alloy [12].

Orbits	Experiment	LDA	LSDA + U	GW [27]	LDA + DMFT
$f_{sh}^{\uparrow}$	150	511	163	174	140
$f_{sh}^{\downarrow}$	150	511	40	25	72
$f_{lh}^{\uparrow}$	612	1590	907	726	619
$f_{lh}^{\downarrow}$	589	1590	597	590	574
$f_{hh}^{\uparrow}$	1273	2479	1592	1642	1637
$f_{hh}^{\downarrow}$	1222	2479	1907	1368	1466
$f_{e\perp}^{\uparrow}$	386	479	333	452	362
$f_{e\perp}^{\downarrow}$	328	479	243	301	306
$f_{e\parallel}^{\uparrow}$	1111	1848	1205	1317	1270
$f_{e\parallel}^{\downarrow}$	941	1848	850	887	1113
n	3.3	7.6	4.1	3.5	3.9

LDA + U, so is the exchange splitting of the electron pockets. In contrast, the hybridization between the As p states and the upper Er f states near the Γ point is rather strong. In LDA + U, the UHB has a strong spin polarization in the minority channel: hybridization thus pushes the corresponding p states away from the Fermi level, leading to too small hole pockets in the minority channel (see Table I). In LDA + DMFT, this spin polarization is smaller and the orbital angular momentum composition of the UHB is different, with larger contributions from components which do not hybridize with p states for symmetry reasons. Hence the smaller exchange splitting of the hole pockets, in better agreement with experiments. It is remarkable that, because of the sensitivity of hybridization effects to both the spin and orbital angular momentum of the $4f$ states, experimental measurements of the exchange splitting of the FS pockets indirectly probe the electronic state of the Er $4f$ shell.

In conclusion, we have shown that a proper description of the electronic structure of RE-V compounds requires a conceptual framework which gives a central role to local atomic physics and multiplet effects, in contrast to conventional frameworks based on one-electron effective descriptions.

TABLE II. Exchange splittings of Shubnikov–de Haas frequencies $\Delta = f^{\uparrow} - f^{\downarrow}$ (in tesla).

Orbits	Experiment[a]	LSDA + U	GW[b]	LDA + DMFT
Δ_{lh}	23	310	136	45
Δ_{hh}	51	315	274	171
$\Delta_{e\perp}$	58	90	151	56
$\Delta_{e\parallel}$	170	355	430	157

[a]Experimental data for an $Er_{0.57}Sc_{0.43}As$ alloy [12].
[b]Chantis *et al.* [27].

This work was supported by the Agence Nationale de la Recherche (France) under the ETSF grant, and by the MRSEC Program of the National Science Foundation under grant No. DMR05-20415. A. G. and L. P. thank the Chemical Bonding Center and the Kavli Institute for Theoretical Physics, UCSB, for hospitality and support. L. P. acknowledges the financial support from ICAM under NSF grant DMR 0645461. We are grateful to A. Gossard for useful discussions.

[1] C. J. Palmstrøm, N. Tabatabaie, and S. J. Allen, Jr., Appl. Phys. Lett. **53**, 2608 (1988).
[2] K. E. Singer *et al.*, Appl. Phys. Lett. **64**, 707 (1994).
[3] D. O. Klenov *et al.*, Appl. Phys. Lett. **86**, 111912 (2005).
[4] B. D. Schultz and C. J. Palmstrøm, Phys. Rev. B **73**, 241407(R) (2006).
[5] W. Kim *et al.*, Phys. Rev. Lett. **96**, 045901 (2006).
[6] C. Kadow *et al.*, Appl. Phys. Lett. **76**, 3510 (2000).
[7] A. G. Petukhov, W. R. L. Lambrecht, and B. Segall, Phys. Rev. B **50**, 7800 (1994).
[8] A. G. Petukhov, W. R. L. Lambrecht, and B. Segall, Phys. Rev. B **53**, 4324 (1996).
[9] S. J. Allen, Jr. F. De-Rosa, C. J. Palmstrom, and A. Zrenner, Phys. Rev. B **43**, 9599 (1991).
[10] R. Bogaerts *et al.*, Physica B (Amsterdam) **177**, 425 (1992).
[11] R. Bogaerts *et al.*, Physica B (Amsterdam) **184**, 232 (1993).
[12] R. Bogaerts *et al.*, Phys. Rev. B **53**, 15 951 (1996).
[13] A. Georges, G. Kotliar, W. Krauth, and M. J. Rozenberg, Rev. Mod. Phys. **68**, 13 (1996).
[14] A. I. Lichtenstein and M. I. Katsnelson, Phys. Rev. B **57**, 6884 (1998); V. I. Anisimov *et al.*, J. Phys. Condens. Matter **9**, 7359 (1997).
[15] D. Vollhardt *et al.*, J. Phys. Soc. Jpn. **74**, 136 (2005).
[16] G. Kotliar *et al.*, Rev. Mod. Phys. **78**, 865 (2006).
[17] J. Hubbard, Proc. R. Soc. A **276**, 238 (1963).
[18] L. V. Pourovskii, B. Amadon, S. Biermann, and A. Georges, Phys. Rev. B **76**, 235101 (2007).
[19] W. T. Carnal, G. L. Goodman, K. Rajnak, and R. S. Rana, J. Chem. Phys. **90**, 3443 (1989).
[20] K. R. Lea, J. M. Leask, and W. P. Wolf, J. Phys. Chem. Solids **23**, 1381 (1962).
[21] S. J. Allen, Jr. *et al.*, Phys. Rev. Lett. **62**, 2309 (1989).
[22] V. I. Anisimov, F. Aryasetiawan, and A. I. Lichtenstein, J. Phys. Condens. Matter **9**, 767 (1997).
[23] P. Larson, W. R. L. Lambrecht, A. Chantis, and M. van Schilfgaarde, Phys. Rev. B **75**, 045114 (2007).
[24] T. Komesu *et al.*, Phys. Rev. B **67**, 035104 (2003).
[25] C. G. Duan *et al.*, Surf. Rev. Lett. **11**, 531 (2004).
[26] J. H. Shim, K. Haule, and G. Kotliar, Nature (London) **446**, 513 (2007).
[27] A. N. Chantis, M. van Schilfgaarde, and T. Kotani, Phys. Rev. B **76**, 165126 (2007).
[28] W. R. L. Lambrecht, B. Segall, A. G. Petukhov, R. Bogaerts, and F. Herlach, Phys. Rev. B **55**, 9239 (1997).
[29] M. Wulff, G. G. Lonzarich, D. Fort, and H. L. Skriver, Europhys. Lett. **7**, 629 (1988).